H2Open Journal

IWA PUBLISHING

H2Open Journal Vol 3 No 1
doi: 10.2166/h2oj.2020.022

Removal of co-existing fluoride, calcium, magnesium, and carbonates, by non-chemical induced electrolysis system for drinking and industrial purposes

A. A. G. D. Amarasooriya* and Tomonori Kawakami

Department of Environmental and Civil Eng., Toyama Prefectural University, 5180 Kurokawa, Imizu-Shi, Toyama 939-0398, Japan

*Corresponding author. E-mail: gayanamarasooriya@gmail.com

Abstract

An electrolysis (ELC) system was proposed to remove co-existing F^-, Ca^{2+}, Mg^{2+}, CO_3^{2-}, and HCO_3^- from groundwater without the addition of any chemicals. The proposed system utilized an ELC cell composed of non-corrosive platinum and stainless steel electrodes. Ion removal mechanisms, performance against different ion concentrations, and charge loading were studied and compared with drinking and industrial water quality guidelines. System performance with real groundwater was also examined. Results revealed that ELC effectively removes ($CO_3^{2-} + HCO_3^-$) in the anode as CO_2, and ($CO_3^{2-} + HCO_3^-$), Ca^{2+}, and Mg^{2+} in cathode as $MgCO_3$, $CaCO_3$, and $Mg(OH)_2$. F^- was removed by co-precipitation with $Mg(OH)_2$ and Coulomb transfer. Maximum removal of 58%-F^-, 42%-Ca^{2+}, and 95%-Mg^{2+} were observed at a charge loading of 1500 C/L. With increasing Ca^{2+} and Mg^{2+}, removal increments of cathode F^-, Ca^{2+}, Mg^{2+}, and ($CO_3^{2-} + HCO_3^-$) were noticed. To meet drinking water guidelines value of 1.5 mg/L of F^-, minimum initial ion concentration ranges should be within $F^- < 4.29$–6 mg/L, $Mg^{2+} < 75$–125 mg/L, $Ca^{2+} > 50$ mg/L, and ($CO_3^{2-} + HCO_3^-$) < 10–0 mmol/L for 1500 C/L. The anode delivered the quality water which meets industrial boiler water alkalinity guideline for the initial ($CO_3^{2-} + HCO_3^-$) < 12.5 meq/L. The community-scale treatment system established in Sri Lanka confirmed smooth operation with a higher removal of F^- and Ca^{2+} in the cathode and ($CO_3^{2-} + HCO_3^-$) in the anode which can be slightly approximated with laboratory results.

Key words: calcium, carbonates, electrolysis removal, fluoride, groundwater, magnesium

INTRODUCTION

The usability of groundwater for domestic and industrial purposes depends upon the water quality. However, the quality of natural groundwater deteriorates day by day, mainly due to the change of natural conditions as well as human and industrial activities. Over the last two decades, fluoride (F^-) occurred by natural pathways was identified as a foremost groundwater contaminant and was reported in more than 20 countries worldwide (Meenakshi & Maheshwari 2006). As per estimates, 200–260 million people from various nations are at dire risk of fluorosis due to the consumption of groundwater abundant in F^- (Ayoob & Gupta 2006; Amini *et al.* 2008). The mineralogical nature of the aquifer material mainly controls the occurrence of F^- in groundwater. According to many studies, either Ca^{2+}, Mg^{2+}, HCO_3^-, CO_3^{2-} (hardness- and alkalinity-causing

H2Open Journal Vol 3 No 1
doi: 10.2166/h2oj.2020.022

agents) ions, or a mixture of those ions have co-existed with F^- ion (Kim & Jeong 2005; Rafique *et al.* 2009; Ketata *et al.* 2011; Rango *et al.* 2012; Salifu *et al.* 2012; Su *et al.* 2013; Singaraja *et al.* 2014; Wickramarathna *et al.* 2017; Karimi *et al.* 2018; Luo *et al.* 2018; Thapa *et al.* 2018). Even though co-existing Ca^{2+}, Mg^{2+}, CO_3^{2-}, and HCO_3^- in drinking groundwater show a non-negative influence on human health, it impacts water palatability and causes scaling problems in both household and industrial equipment (Zhi & Zhang 2016). Therefore, not only F^- but also co-existed Ca^{2+}, Mg^{2+}, CO_3^{2-}, and HCO_3^- removal are essential to meet the standards for drinking and industrial water quality.

The most common technologies for removing coexisting F^-, Ca^{2+}, Mg^{2+}, HCO_3^-, and CO_3^{2-} in industrial and drinking purposes are reverse osmosis (RO), nanofiltration (NF), ion exchange (IE), chemical treatment (CT), as well as two electrochemical methods, electrochemical precipitation (ECP) and electrodialysis (ELD) (Gascó & Méndez 2005; Gabrielli *et al.* 2006; Kuokkanen *et al.* 2013; Shen & Schafer 2014; Zhi & Zhang 2016; Janson *et al.* 2018). However, except for RO, NF, and ELD, the main disadvantage of IE, CT, and ECP methods are that they need to introduce extra chemicals or they release extra ions into the water during the treatment process. Besides, RO, ELD, and NF are complicated in technology, cost-ineffective, and quantity of water rejections are high. Therefore, RO, ELD, and NF are not suitable for water-scarce regions and developing nations expecting lower unit costs for groundwater purification.

However, ECP technology, electrocoagulation (EC) overcomes the above problems. It attracts much attention as a process for removing coexisting Ca^{2+}, Mg^{2+}, HCO_3^-, CO_3^{2-} as well as F^- since EC operation can be performed with minimal cost and minimal chemicals introduction to the source water (Zeppenfeld 1998, 2011; Gabrielli *et al.* 2006; Zhi & Zhang 2016). However, the introduction of chemicals is the major drawback of EC since it affects the final water quality and operational costs. So far, none of the ECP or EC studies were found to avoid any chemical addition in F^- or coexisting Ca^{2+}, Mg^{2+}, HCO_3^-, or CO_3^{2-} removal. Therefore, developing an ECP or EC system without any chemical addition that removes coexisting F^-, Ca^{2+}, Mg^{2+}, HCO_3^-, and CO_3^{2-} will be attractive to the scientific community. Moreover, it can be beneficial to developing nations seeking low-cost and effective technology to meet both industrial and drinking water quality guidelines.

Usually, ECP's EC is performed in a communal cell reactor and using a high pH environment around the cathode to facilitate the removal of ions by coagulation. Dissociation of anode material provides a coagulation agent to the solution for Ca^{2+}, Mg^{2+}, HCO_3^-, CO_3^{2-} as well as F^- removal. Therefore, by using a communal cell EC reactor, as well as a corrosive anode, the chemical introduction cannot be controlled or terminate appropriately. However, by separating the anode and the cathode electrodes using a diaphragm (with simple electrolysis (ELC) cell configuration) and utilizing non-corrosive anode (platinum (Pt)) introduction of the chemical can be stopped. Also, ELC cell configuration allows the maintenance of adequate pH, prevent mixing the anode and the cathode solutes as well as the transference of positive and negative ion through a diaphragm similarly to ELD without any specific ion selectivity. Moreover, ELC ion-removal technologies were reported only a few times in our previous studies, and only for F^- removal (Kawakami *et al.* 2018; Amarasooriya & Kawakami 2019).

Therefore, the main objective of this study was to explore the removal of co-existing F^-, Ca^{2+}, Mg^{2+}, CO_3^{2-}, and HCO_3^- from groundwater by ELC. The system's performance against charge loading and various initial concentrations of F^-, Ca^{2+}, Mg^{2+}, CO_3^{2-}, and HCO_3^- were studied on a laboratory scale. The proposed system performance and stability were studied on a community scale as well in the northern part of Sri Lanka where the groundwater was highly contaminated with F^-, Mg^{2+}, and Ca^{2+}, and with $HCO_3^- + CO_3^{2-}$ for drinking purposes.

H2Open Journal Vol 3 No 1
doi: 10.2166/h2oj.2020.022

MATERIAL AND METHODS

Experimental and field-scale ELC cell configuration

The ELC reactor design was adopted from our previous studies (Amarasooriya & Kawakami 2019). Accordingly, as an ELC reactor for the laboratory experiments, a tank made of transparent acrylic resin material was used (length 20 cm × height 10.2 cm × width 5 cm). The tank was divided into two equal volumes (effective volume 490 mL) cells with a 2 mm thick (effective area: 20 cm × 10.2 cm) commercial ceramic diaphragm F-C1 (Nikkato Corp., Japan). This diaphragm helped to separate the anode solution from the cathode solution, facilitated the transference of ions between cells without any selectivity, and prevented the mixing of sludge formed in the cathode (Figure 1). To increase the length of the water flow, individual cells were further divided into two equal slots with an acrylic plate, keeping open 10 mm from the bottom. U-shaped stainless steel (SS) (Effective length = 30 cm, $\varphi = 1.00$ mm) and platinum (Pt) (effective length = 30 cm, $\varphi = 0.40$ mm) wires were used as electrodes for the cathode and the anode, respectively. The distance between electrodes was kept as 3.3 cm. The assembly was connected to a constant current power supply for all experiments, and inflow rates were kept at 10 mL/min for both the anode and the cathode in all experiments. The ELC system employed for the laboratory and field experiments is shown in Figure 2.

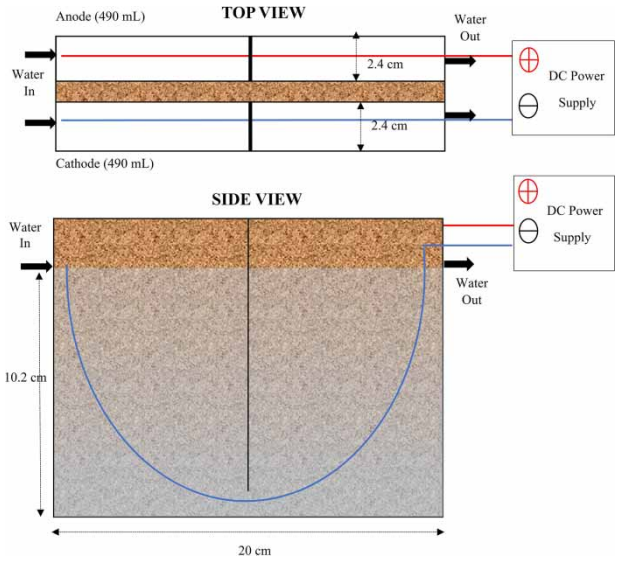

Figure 1 | Electrolysis cell configuration.

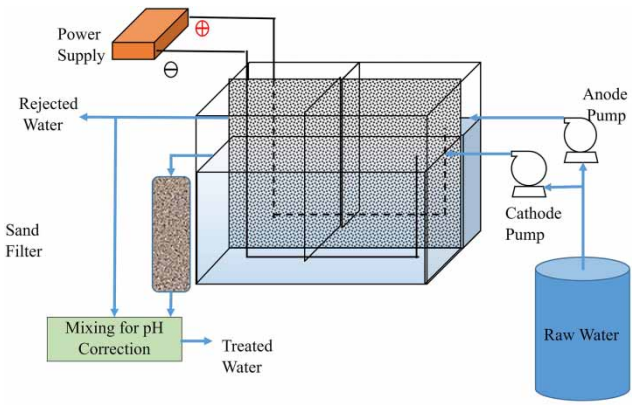

Figure 2 | Electrolysis system.

H2Open Journal Vol 3 No 1
doi: 10.2166/h2oj.2020.022

For the community-scale treatment system, series-connected two reactors made out of the same material similar to that of the laboratory experimental ELC reactor were utilized. The effective total volume of the anode and the cathode was 12 L (28 cm × 40 cm × 5.357 cm × 2) and equivalent with the laboratory scale system's resident time (0.77 hr). U shaped Pt wires (30 cm × 2) and SS mesh (2 cm × 2 cm) with a size of 24 cm × 36 cm × 2 were used as anode and cathode electrodes, respectively.

Operational conditions, sample collection, and storage

For the experiments, a series of F^-, Mg^{2+}, Ca^{2+}, and ($HCO_3^- + CO_3^{2-}$) spiked tap water (hereafter initial concentrations will be denoted as F_0^-, Mg_0^{2+}, Ca_0^{2+}, and $(HCO_3^- + CO_3^{2-})_0$) was used as synthetic groundwater. The initial ion concentrations were selected so that it exceeds the Sri Lankan and WHO recommended drinking water guideline values. By applying a constant current to the immersed SS and Pt electrodes, synthetic groundwater was pumped continuously to the ELC reactor anode and cathode. Electrolysis time (Current applied for unit flow rate ampere per (liter per second) = (A/(L/s))) or charge loading (Coulomb per liter = C/L) are the key parameters that affected ion removal efficiencies. Accordingly, by changing the applied current, different charge loadings were applied to the system. The initial ion concentrations flow rates and the applied charge loading for the various experiments were summarized in Table 1.

A groundwater source located in Sri Lanka's Medawachchiya area (8°32′02.8″N 80°29′57.6″E) of the Anuradhapura District was selected for the field study. Samples were collected after three hours of system stabilizing time from ELC reactor anode and cathode outlets. The Anode and the Cathode pH stability was considered for the system stabilization point determination. Both water samples from the field and the laboratory were filtered with 0.45 μm pores membrane filter to eradicate bacteriological activities affecting the water quality and to remove non-dissolved particles. Collected samples from the field and laboratory were stored into 50 mL polyethylene bottles on location and analyzed within the 45 days of their collection in Japan. For the isotherm experiments, precipitates in the cathode of the ELC was filtered and dried at 70 °C for 4 hours. Dried samples were weighed and transferred to the 50 mL polyethylene tubes containing 10 mg/L F^- solution. Samples were then shaken in an electrical shaker for 0.77 hours (similar to the resident time of the cathode). After 0.77 hours, samples were filtered with a membrane filter with 0.45 μm pores to the 50 mL polyethylene bottles until the analysis was performed.

Chemicals and instruments

Chemicals purchased from Wako Chemicals from Japan were used for preparing artificial groundwater. The platinum electrode for anode was bought from the Nilaco Corporation, Japan, and a stainless steel electrode for cathode was purchased from the local market in Japan. Anions were analyzed using an ion chromatograph (Thermo ICS-2000; Thermo Scientific, USA) with separation column (IonPac AS18; Thermo Scientific, USA) and eluent: KOH 23–40 mmol/L gradient was used. Cations were analyzed using an ion chromatograph (Thermo ICS-1500; Thermo Scientific, USA) with separation column (Ion Pac CS12 Thermo Scientific, USA) and eluent (MSA 30 mmol/L isocratic; Thermo Scientific, USA) was used. The calibration standard solution after every 20 samples was analyzed for the observation of the stability of the ion chromatographic detector. If the overall concentration variability of the examined calibration standard solution was not below 5%, a re-analysis of the samples and standards were performed. X-ray diffraction (XRD) analysis of the precipitates was performed with a RIGAKU MiniFlex (Japan) machine equipped with CuK-Alpha radiation (configuration: 2 theta/min 30 KV, 15 mA (450 W)). The

Table 1 | Operational conditions and initial concentrations maintained at the laboratory and field experiments

Laboratory conditions

			Initial concentrations				Inflow rate (mL/min)		Outflow rate (mL/min)	
Versus ion removal/experiment	**Charge loading (C/L)**	**Current (A)**	**F^- (mg/L)**	**Mg^{2+} (mg/L)**	**Ca^{2+} (mg/L)**	**$HCO_3^- + CO_3^{2-}$ (mmol/L)**	**Anode**	**Cathode**	**Anode**	**Cathode**
Charge loading	0–1500	0–0.25	10	100	100	10	10	10	10	10
Anode flow rate	1500	0.25	10	100	100	10	2.5–20	10	2.5–20	10
F_0^-	1500	0.25	5–20	100	100	10	10	10	10	10
Mg_0^{2+}	1500	0.25	10	0–125	100	10	10	10	4–10	14–10
Ca_0^{2+}	1500	0.25	10	100	0–125	10	10	10	8–10	12–10
$(HCO_3^- + CO_3^{2-})_0$	1500	0.25	10	100	100	0–12.5	10	10	10	10

Field conditions

	Charge loading (C/L)	**Current (A)**	**F^- (mg/L)**	**Mg^{2+} (mg/L)**	**Ca^{2+} (mg/L)**	**$HCO_3^- + CO_3^{2-}$ (mmol/L)**	**Anode**	**Cathode**	**Anode**	**Cathode**
Average	1324	5.74	2.71	130.8	54.7	13.8	260	260	260	260

H2Open Journal Vol 3 No 1
doi: 10.2166/h2oj.2020.022

H2Open Journal Vol 3 No 1
doi: 10.2166/h2oj.2020.022

pH measurements were conducted with the glass electrode method (Orion Star A324; Thermo Scientific, USA). Voltage logging for calculating applied current and charge loading in a community-scale treatment system was performed with a data logger (ONSET, HOBO). As a power source, a constant voltage power supply (max 10 A) was used.

RESULTS AND DISCUSSION

Process description and ion removal mechanisms

As electrolysis proceeded, H^+ ions produced in the anode cell create a low pH environment (Equation (1)) while OH^- ions produced in the cathode cell and caused a high pH environment (Equation (4)). In the anode, HCO_3^- and CO_3^{2-} should be removed as carbon dioxide by reacting with H^+ (Equations (2) and (3)). The majority of ions could be removed in the cathode by reacting either with CO_3^{2-} or OH^- (Equations (5)–(9)).

The anode reactions:

$$H_2O(l) \rightarrow \frac{1}{2}O_2(g) + 2H^+(aq) + 2e^- \quad (1)$$

$$HCO_3^-(aq) + H^+ \overset{K_1=4.448\times10^{-7}}{\rightleftharpoons} H_2CO_3(aq) \rightarrow CO_2(g)\uparrow + H_2O(l) \quad (2)$$

$$CO_3^{2-}(aq) + 2H^+ \rightarrow CO_2(g)\uparrow + H_2O(l) \quad (3)$$

The cathode reactions:

$$2H_2O(l) + 2e^- \rightarrow 2OH^-(aq) + H_2(g) \quad (4)$$

$$HCO_3^-(aq) + OH^- \overset{K_2=4.690\times10^{-11}}{\rightleftharpoons} CO_3^{2-}(aq) + H_2O(l) \quad (5)$$

$$CO_3^{2-}(aq) + Ca^{2+}(aq) \overset{Ksp=3.3\times10^{-9}}{\rightleftharpoons} CaCO_3(s)\downarrow \quad (6)$$

$$CO_3^{2-}(aq) + Mg^{2+}(aq) \overset{Ksp=1.6\times10^{-8}}{\rightleftharpoons} MgCO_3(s)\downarrow \quad (7)$$

$$Mg^{2+}(aq) + 2OH^-(aq) \overset{K_{sp}=5.61\times10^{-12}}{\rightleftharpoons} Mg(OH)_2(s)\downarrow \quad (8)$$

$$Ca^{2+}(aq) + 2OH^-(aq) \overset{Ksp=5.02\times10^{-6}}{\rightleftharpoons} Ca(OH)_2(s)\downarrow \quad (9)$$

To verify the described removal mechanisms in the cathode, XRD analysis was performed for the precipitates collected from the cathode for charge loading of 1500, 1250, and 1000 C/L. The XRD pattern showed only the presence of $CaCO_3$, $MgCO_3$, and $Mg(OH)_2$ (Figure 3). According to the peak intensities; the predominant mineral phase of $CaCO_3$ was calcite; nevertheless, the aragonite mineral phase was found significantly. In comparison, the peak intensities of $CaCO_3$ and $MgCO_3$ decreased with decreasing charge loading; thus, crystallinity seems to be reduced due to the formation of $Mg(OH)_2$.

Due to the higher pH environment in the cathode, Mg^{2+}, F^-, Ca^{2+}, and $(HCO_3^- + CO_3^{2-})$ ions start precipitating, which could be involved in removing F^- (Equations (10)–(13)). Moreover, the applied current-generated Coulomb's force could be an advantage for ion transfer between the

H2Open Journal Vol 3 No 1
doi: 10.2166/h2oj.2020.022

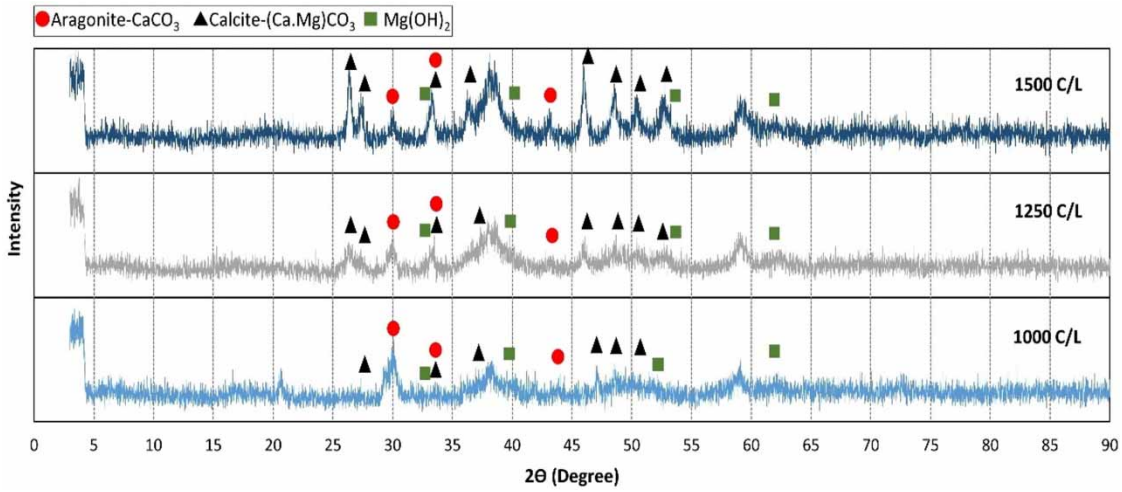

Figure 3 | XRD patterns of precipitates collected from various C/Ls.

cathode and the anode. Accordingly, plausible F^- removal mechanisms can be presented as Equations (11)–(13)

$$xMg^{2+}(aq) + (2z - y)OH^-(aq) + yF^-(aq) \rightarrow Mg_xF_y(OH)_{2z-y}(s) \downarrow \text{(co-precipitation)} \quad (10)$$

$$Mg^{2+}(aq) + 2F^-(aq) \overset{ksp=5.16\times10^{-11}}{\rightleftharpoons} Mg(F)_2(s) \downarrow \quad (11)$$

$$Ca^{2+}(aq) + 2F^-(aq) \overset{ksp=3.45\times10^{-11}}{\rightleftharpoons} Ca(F)_2(s) \downarrow \quad (12)$$

$$(Ca.Mg)(CO_3)_2(s) + xF^-(aq) \rightleftharpoons (Ca.Mg)(CO_3)_{2-x}F_x \downarrow + x\,CO_3^{2-}\text{(adsorption)} \quad (13)$$

The absence of MgF_2 and CaF_2 peaks in XRD (Figure 3) revealed that fluoride could be removed by either adsorption or co-precipitation, with predominantly formed $CaCO_3$, $MgCO_3$, and $Mg(OH)_2$. Turner *et al.* (2005) reported that $CaCO_3$ has a high affinity for removing F^- ion by surface adsorption dependent on the $CaCO_3$ surface area. Furthermore, Masindi *et al.* (2015) investigation suggested that cryptocrystalline $MgCO_3$ could effectively remove F^- by adsorption (Turner *et al.* 2005; Masindi *et al.* 2015). However, ELC experiments cathodes maintained high pH values than that of those studies; therefore, the possibility of adsorptive F^- removal was verified with adsorptive experiment.

Precipitates generated in the absence of F^- under the experiment conditions (listed in Table 1) were collected, and adsorption isotherm was performed with F^- water (Figure 4). The Freundlich isotherm was found to be the best fit for the results. In Figure 4, C is F^- concentration in the solution expressed in a unit of mg/L. Q is the adsorption capacity (mg/g) at a specific concentration of F^-. According to the Freundlich isotherm, the F^- adsorption capacity was 0.60 mg/g at the F^- concentration of 3.52 mg/L. By assuming total Ca^{2+} and Mg^{2+} (107.2 and 65.62 mg/L; section 'Effect of charge loading on ion-removal efficiencies'; Figure 5(a), removal at 1500 C/L) were removed either as $CaCO_3 + MgCO_3$ or $CaCO_3 + Mg(OH)_2$, as well as F^- was removed only by adsorption (4.88 mg/L; Figure 5(a), removal at 1500 C/L), F^- adsorption capacity by ($CaCO_3 + MgCO_3$) and ($CaCO_3 + Mg(OH)_2$) can be calculated as 8.15 and 9.42 mg/g respectively. These calculated adsorptive values were much higher than the Freundlich isotherm, given the F^- adsorption capacity of 0.60 mg/g. Therefore, it can be concluded that the fraction of F^- adsorbed by a mixture of $CaCO_3$, $MgCO_3$, and $Mg(OH)_2$ was not significant. Therefore, another precipitative F^- removal mechanism should be incorporated to remove the F^-.

H2Open Journal Vol 3 No 1
doi: 10.2166/h2oj.2020.022

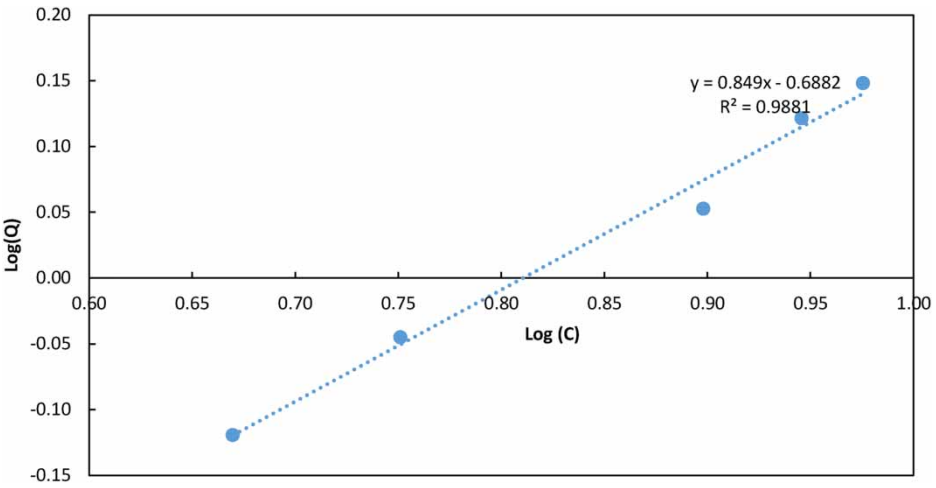

Figure 4 | Freundlich isotherm for the precipitate collected from ELC without F^-.

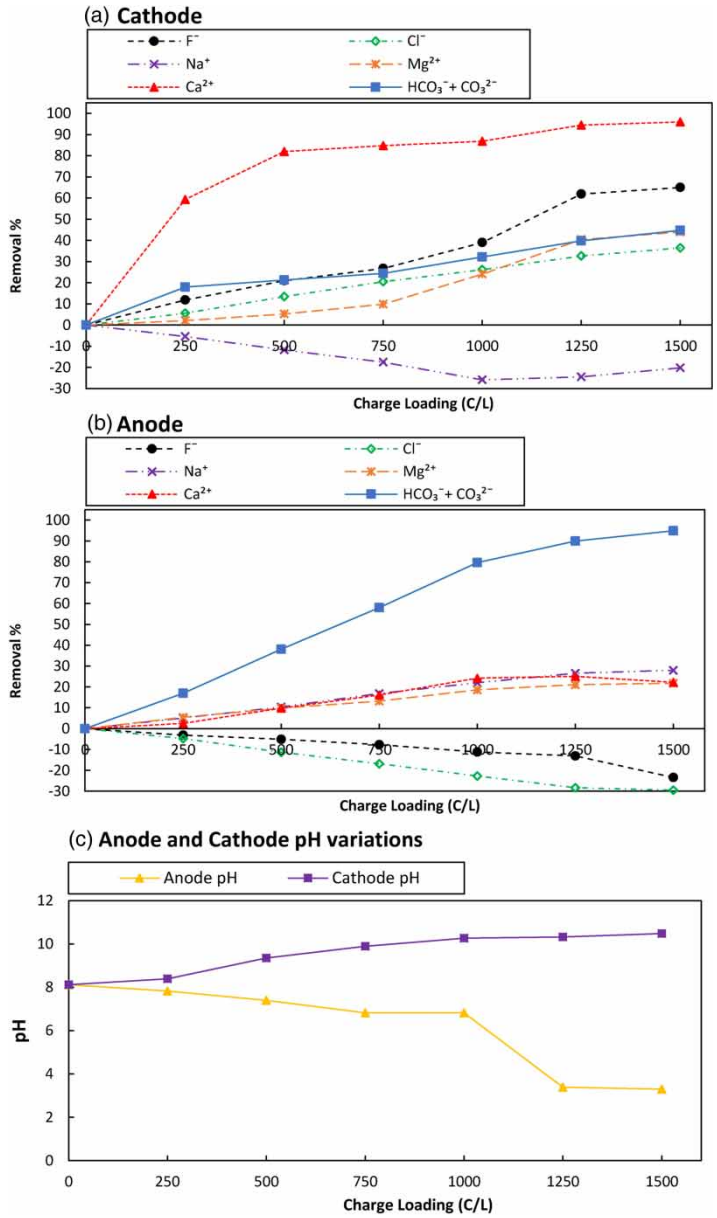

Figure 5 | Influence of the charge loading in the electrolytes on the ion removal and pH. (a) Cathode, (b) anode, (c) pH variation; $F_0^- = 10$ mg/L, $Ca_0^{2+} = 100$ mg/L, $Mg_0^{2+} = 100$ mg/L, and $(HCO_3^- + CO_3^{2-})_0 = 10$ mmol/L.

H2Open Journal Vol 3 No 1
doi: 10.2166/h2oj.2020.022

Kawakami *et al.* (2018) proposed that F^- co-precipitation occurred by $Mg(OH)_2$ (Kawakami *et al.* 2018). Besides, previous studies of the de-fluoridation of water using nano-magnesium oxide suggested that F^- exchange between $Mg(OH)_2$'s OH^- and F^- could take place due to the isoelectric nature and the similar radius of F^- and OH^- ions (Devi *et al.* 2012; Oladoja *et al.* 2016), and the co-precipitation mechanism for F^- removal by $Mg(OH)_2$ was proposed by Devi *et al.* (2012). Accordingly, F^- removal mainly took place by co-precipitation with $Mg(OH)_2$ other than the adsorption to the $CaCO_3 + MgCO_3$, and by Coulomb force transfer to the anode.

Effect of charge loading on ion-removal efficiencies

After three hours of ELC stabilizing time, flow through the diaphragm was found to be negligible, and ion removal percentages were calculated without further corrections. Due to the diprotic nature of carbonic acid (H_2CO_3) in the solution, both CO_3^{2-} and HCO_3^- exist, and their concentrations change with the solution's pH. Therefore, the sum of the carbonate (HCO_3^- and CO_3^{2-}) concentrations (hereafter $(HCO_3^- + CO_3^{2-})$) as mmol/L accounts for the alkalinity. The charge of water samples $(HCO_3^- + CO_3^{2-})$ was calculated by accounting for the system's ion charge balances. Trace ion concentrations were neglected, and the calculation focused on major ions in Equation (14). For calculating HCO_3^- and CO_3^{2-} concentrations as mmol/L, as described in Equations (19) and (18), the carbonates' charge balance equation (Equation (15)) and $HCO_3^- \leftrightarrow CO_3^{2-}$ equilibria (Equations (16) and (17)) were employed. The $K_2 = 4.69 \times 10^{-11}$ (mol/L) (value was taken from the findings of Plummer & Busenberg (1982)).

$$(T_C) = \text{Total charge of } CO_3^{2-} \text{ and } HCO_3^-$$
$$= (\text{the sum of cation charge} - \text{the sum of anion charge except for } CO_3^{2-} \text{and } HCO_3^-)$$

$$\{2[\mathbf{CO}_3^{2-}] + [\mathbf{HCO}_3^-]\}(\mathbf{eq/L}) = \{[H^+] + [Na^+] + [NH_4^+] + [K^+] + 2[Mg^{2+}] + 2[Ca^{2+}]\}$$
$$-\{[OH^-] + [F^-] + [Cl^-] + 2[SO_4^{2-}] + [NO_3^-]\}(eq/L) \quad (14)$$

The charge balance for CO_3^{2-} and HCO_3^- can be written as (assuming no dissociation of atmospheric CO_2 (g))

$$T_C = 2[CO_3^{2-}] + [HCO_3^-] \quad (eq/L) \quad (15)$$

$HCO_3^- \leftrightarrow CO_3^{2-}$ equilibria:

$$HCO_3^-(aq) \overset{K_2 = 4.690 \times 10^{-11}}{\rightleftharpoons} CO_3^{2-}(aq) + H^+(aq) \quad (16)$$

$$K_2 = \frac{[CO_3^{2-}] \times [H^+]}{[HCO_3^-]} \quad (17)$$

By rearranging Equation (17),

$$CO_3^{2-} = \frac{K_2\,[HCO_3^-] \times 10^3}{[H^+]}(mol/L) \quad (18)$$

H2Open Journal Vol 3 No 1
doi: 10.2166/h2oj.2020.022

By substituting CO_3^{2-} in Equation (15) for Equation (18),

$$HCO_3^- = \frac{T_C \times 10^3}{1 + \left(\frac{2K_2}{[H^+]}\right)} (\text{mol/L}) \quad (19)$$

Figure 5 shows the effect of charge loading (0–1500 C/L) on ion removal and related pH under the initial conditions described in Table 1. According to that plot, the highest F^-, Mg^{2+}, Ca^{2+}, Cl^-, and $(HCO_3^- + CO_3^{2-})$ removal efficiencies 65, 96, 44, 36, and 45%, respectively were achieved at 1500 C/L charge loading in the cathode. Hence, for further experiments, 1500 C/L was selected. According to the cathode ion removal, higher charge loading resulted in removing F^-, Mg^{2+}, Ca^{2+}, and Cl^- positively and Na^+ negatively from the cathode. The ELC reactor generates an electric field between its electrodes; thus, charged particles experience a force (hereafter Coulomb force) according to Coulomb's law, which results in the movement of ions. Therefore, Na^+ was transferred by Coulomb forces to the cathode from anode which caused negative removal in the anode. Na^+ removal in the anode showed positive removal since it transferred to the cathode. The positive removal of the Cl^- ions in the cathode was obviously due to transfer by Coulomb force to the anode, which can be seen in Figure 5(b) as a negative removal in the anode. However, the difference between Cl^- removal in the cathode and the anode was non-negligible and increased from 1 to 7% for 250 to 1500 C/L, respectively. With ion chromatographic analysis, the presence of the OCl^- ion was confirmed. Usually, Cl_2(g) react with water molecules and form the hypochlorous acid (HOCl) which has added advantages to the ELC system since it can disinfect the water. Accordingly, Cl^- should be removed as Cl_2 (g) in the anode, which caused a 1–7% difference between Cl^- removal in the cathode and the anode.

Due to the electron acquisition for Cl_2(g) generation, H^+ and OH^- production was evidently reduced in the ELC reactor. Calculated OH^- and H^+ based on the introduced charge loading (Equation (20)) and based on the $Mg(OH)_2$ precipitated, and the CO_3^{2-} and CO_2 formed are shown in Table 2. According to the results, OH^- and H^+ concentrations calculated in both ways were very similar except for the 1500 C/L charge loading. The Coulomb force transfer of H^+ and OH^- between anode and cathode resulted in neutralization and caused this deviation. Moreover, H^+ and OH^- concentrations calculated based on $Mg(OH)_2$ precipitated and CO_3^{2-} and CO_2 formed were very similar in anode and cathode, exhibiting a slight increment for the charge loading of 1250–1500 C/L. The increase of Coulomb forces contributes to high H^+, and OH^- neutralization could be the reason. On the other hand, an increase in the charge loading >1250 C/L slightly affects

Table 2 | H^+ and OH^- calculated with Equation (20) and experimental results

Charge loading (C/L)	Calculated with Equation (20) (mol/L)			Calculated with experimental results (mol/L)	
	Cl^- removed	H^+	OH^-	H^+	OH^-
250	0.00070	0.0019	0.0019	0.0016	0.0023
500	0.00088	0.0043	0.0043	0.0033	0.0044
750	0.00107	0.0067	0.0067	0.0054	0.0066
1000	0.00104	0.0093	0.0093	0.0081	0.0095
1250	0.00116	0.0118	0.0118	0.0096	0.0110
1500	0.00092	0.0146	0.0146	0.0107	0.0113

H2Open Journal Vol 3 No 1
doi: 10.2166/h2oj.2020.022

the removal of Mg^{2+} and F^- ions.

$$OH^-/H^+ \text{ introduced } \left(\frac{\text{mol}}{L}\right) = \frac{\text{Charge Loading } \left(\frac{C}{L}\right)}{\text{Faraday constant } (96485.33)(C/\text{mol})} - \text{Total Cl removed from both anode and cathode } \left(\frac{\text{mol}}{L}\right) \quad (20)$$

According to Figure 5(a), removal of ($HCO_3^- + CO_3^{2-}$) increased marginally over the increasing charge loading, likely transferred to the anode by Coulomb force. The increase in the removal of Mg^{2+}, Ca^{2+} and ($HCO_3^- + CO_3^{2-}$) with increasing charge loading in the cathode occurred due to the increase in OH^- production. Mainly, groundwater was used as boiler water in industrial requirements. American Boiler Manufacturers Association (ABMA) and the Japan International Cooperation Agency's alkalinity guideline for boiler water was 50–400 mg/L and 1–8 meq/L as $CaCO_3$ (Electric Power Development Co. *et al.* 2013). Safe levels of F^-, Mg^{2+}, Ca^{2+}, and $HCO_3^- + CO_3^{2-}$ recommended by the World Health Organization (WHO)'s guidelines for drinking water were 1.5, 50, 75 mg/L, and 6.1 mmol/L, respectively. According to the results, maximum removal (at a charge loading of 1500 C/L) was only good enough to remove Ca^{2+} and $HCO_3^- + CO_3^{2-}$ from the cathode to meet the guideline value for drinking water. However, $HCO_3^- + CO_3^{2-}$ reduced in the anode was able to meet both industrial and drinking water quality guidelines. However, depending on the initial water quality and the expected guideline values, either anode water or cathode water should be discarded. To minimize the discarding water quantity, flow rate vs. ion removal was examined in detail, as discussed in section 'Effect of the anode flow rate on ion removal'.

Effect of the anode flow rate on ion removal

To minimize the rejected water quantity and to find the best ion removals, the anode outflow rate variation with a constant cathode outflow rate was studied under Table 1 conditions. Figure 6 illustrates the removal of ions in the cathode (Figure 6(a)), those in the anode (Figure 6(b)), and pH variations in the anode and the cathode (Figure 6(c)). According to Figure 6(a), the removal of Ca^{2+}, Mg^{2+}, and $HCO_3^- + CO_3^{2-}$ reached its maximum in 10, 15, and 15 mL/min of the anode flow rates, respectively. Fluoride removal reached its maximum at the anode flow rate of 20 mL/min. However, in the range of anode flow rate 5–20 mL/min, F^- removal increased marginally due to the slight removal increment of Mg^{2+}. With increasing anode flow rate, the charge loading and H^+ generation in the anode decreases, resulting in CO_2 generation decrease as well as decrees of OH^- neutralizing in the cathode. That causes the $HCO_3^- + CO_3^{2-}$ removal decrees in the anode as well as the slight removal increment of Mg^{2+} in the cathode. Accordingly, the anode flow rate around 10 mL/min was found better for maximizing the F^-, Mg^{2+}, and Ca^{2+} removal in the cathode, and ($HCO_3^- + CO_3^{2-}$) removal in the anode by minimizing the rejected water quantity. Therefore, the anode flow rate of 10 mL/min was selected for further experiments.

Effect of initial F^- concentration on ion removal

Removal of the F^- is crucial for the drinking water treatment, and this section describes the effect of initial F^- (F_0^-) concentration on F^- and other ion removals. After three hours of ELC time, flow through the diaphragm was found negligible, and ion removal percentages were calculated without concentration correction. As shown in Figure 7(a), removal of F^- decreased slightly from 66% to 58% as F^- increased presumably, due to the F^- co-precipitation increment.

H2Open Journal Vol 3 No 1
doi: 10.2166/h2oj.2020.022

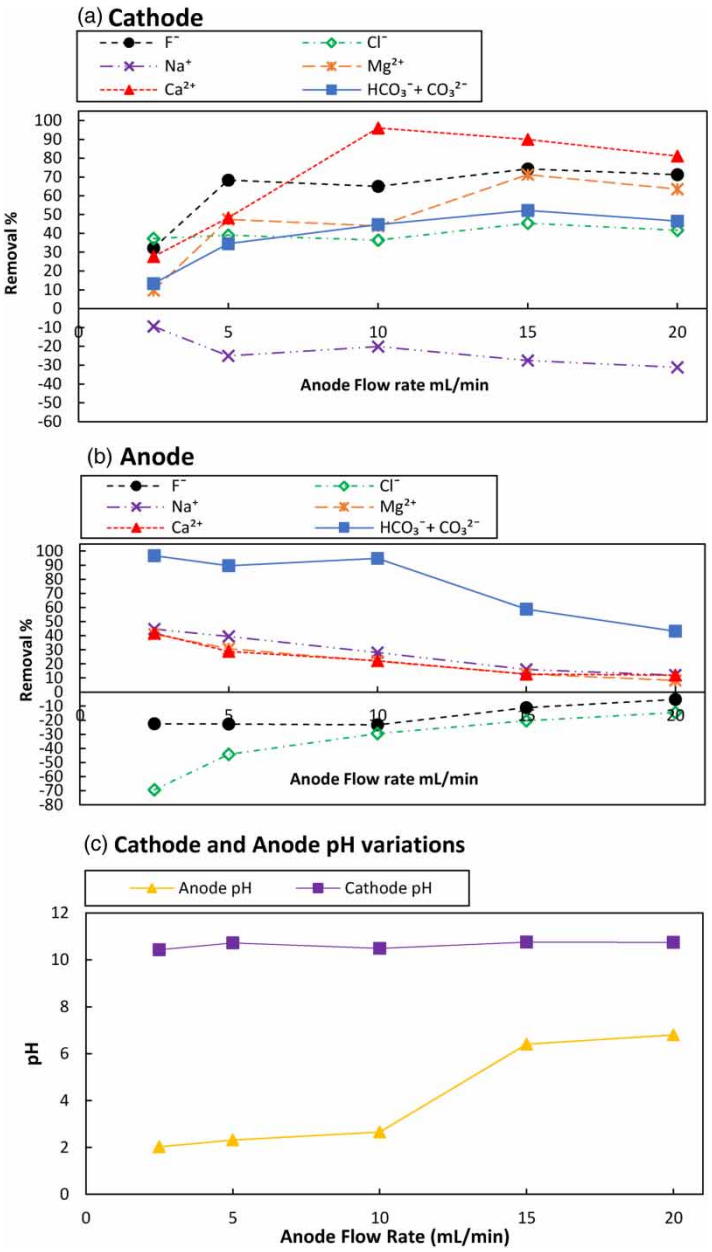

Figure 6 | Influence of the anode flow rate in the electrolytes on the ion removal percentage and pH. (a) Cathode, (b) anode, (c) pH variation; cathode flow rate 10 mL/min, $F_0^- = 10$ mg/L, $Ca_0^{2+} = 100$ mg/L, $Mg_0^{2+} = 100$ mg/L, and $(HCO_3^- + CO_3^{2-})_0 =$ 10 mmol/L, 1500 C/L.

The higher concentration of F_0^- ion, which replaces OH^- ion in the precipitate due to increased competition between OH^- and F^- due to the similar radius, causes an increment of F^- ion co-precipitation. The same observation was described in Kawakami *et al.* (2018) study. Furthermore, the Coulomb transfer of F^- to the anode was noticed and found constant over the increasing F_0^- due to no change of the charge loading (Figure 7(b)). Also, no significant change in the removal rates of, Ca^{2+}, Mg^{2+}, $(HCO_3^- + CO_3^{2-})$, Na^+ and Cl^-, and no pH changes were observed in both the anode and the cathode with increasing F_0^- obviously, due to no change in applied charge loading. According to the F^- removal trend in the cathode, F^- removal for $F_0^- < 5$ mg/L will not be reduced by less than 66%. By accounting 66% removal of F^-, maximum $F_{0,}^-$ which can be treated to meet the drinking water quality guideline, can be calculated. Accordingly, a maximum of 4.29 mg/L F_0^- can be treated to meet the WHO guideline of 1.5 mg/L. However, the calculated value was valid only

H2Open Journal Vol 3 No 1
doi: 10.2166/h2oj.2020.022

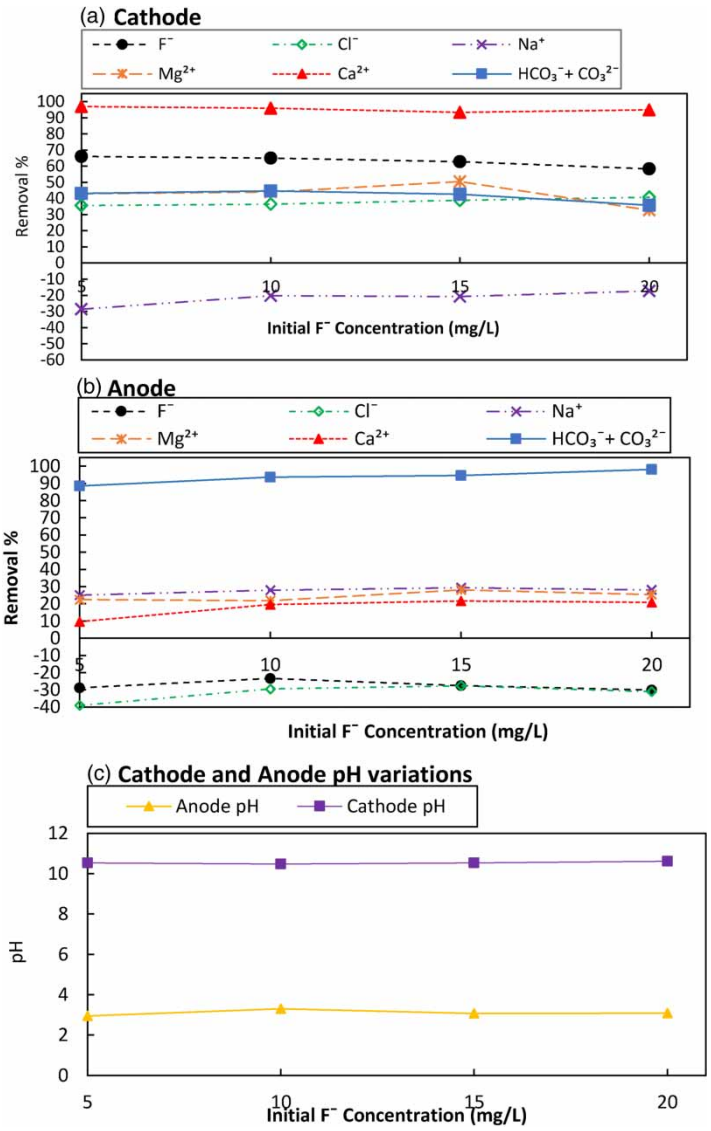

Figure 7 | Influence of the initial F^- concentration in the electrolytes on the ion removal percentage the and pH. (a) Cathode, (b) anode, (c) pH variation; $F_0^- = 0$–20 mg/L, $Ca_0^{2+} = 100$ mg/L, $Mg_0^{2+} = 100$ mg/L, and $(HCO_3^- + CO_3^{2-})_0 = 10{,}000$ μmol/L, 1500 C/L.

for the initial Mg^{2+} (Mg_0^{2+}) concentration of 100 mg/L used in this experiment. For lower Mg_0^{2+}, the same removal percentage may be possible. Therefore, the effect of Mg_0^{2+} on F^- removal is studied in detail in section 'Effect of the initial Mg^{2+} concentration on ion removal'.

Effect of the initial Mg^{2+} concentration on ion removal

This section describes the effect of the initial Mg^{2+}(Mg_0^{2+}) concentration (0–125 mg/L) on ELC ion removal under the experimental conditions described in Table 1. After three hours of system stabilization, flow through the diaphragm was observed as 4.20, 3.66, 3.16, 1.99, 0, and 0 mL/min from the anode to the cathode, respectively, for Mg_0^{2+} concentrations of 0, 25, 50, 75, 100, and 125 mg/L. Accordingly, the removal percentage was calculated by accounting the inflow weight and outflow weight of the elements.

According to Figure 8(a) and 8(b), it is clear that even in the absence of Mg^{2+}, F^- was removed from the cathode by both precipitation (6.9%) (adsorbed to the $CaCO_3$) and Coulomb's transfer to the anode (19.4%). For $Mg_0^{2+} > 50$ mg/L, the removal of F^- increased sharply and became mostly

H2Open Journal Vol 3 No 1
doi: 10.2166/h2oj.2020.022

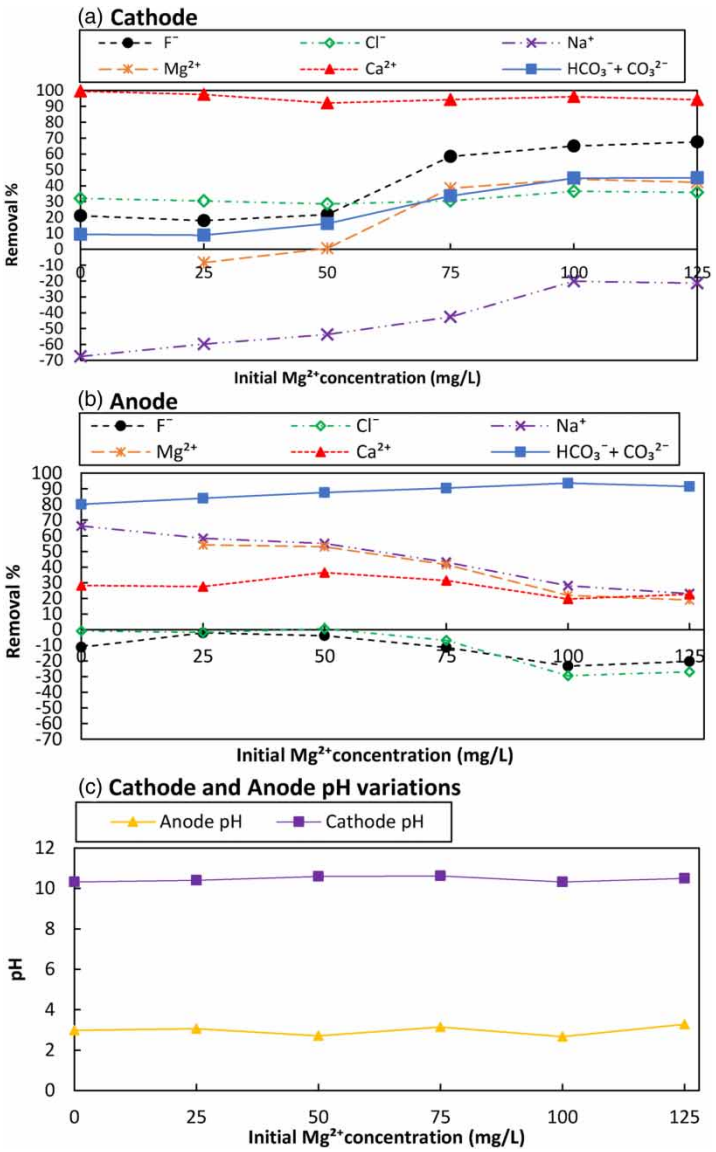

Figure 8 | Influence of the initial Mg^{2+} concentration in the electrolytes on the ion removal percentage and pH. (a) Cathode, (b) anode, (c) pH variation; $F_0^- = 10$ mg/L, $Ca_0^{2+} = 100$ mg/L, $Mg_0^{2+} = 0$–125 mg/L, and $(HCO_3^- + CO_3^{2-}) = 10$ mmol/L, 1500 C/L.

steady (58–67%) in the range of Mg_0^{2+}, 75–125 mg/L. Since OH^- was limited in the reactor, the increase of Mg^{2+} removal (Mg_0^{2+}–Mg^{2+}) varies slightly according to the solubility product calculation ($(Mg^{2+}) = KSp/(OH^-)^2$). However, even in the highest Mg_0^{2+} concentration, the system was unable to remove sufficient F^- to meet the WHO guideline. Therefore, both Mg_0^{2+} and F_0^- concentrations in groundwater, as well as applied charge loading, should be balanced to meet guideline values. However, with the above limitations and results, minimal Mg_0^{2+} required to treat $F_0^- = 4.29$ mg/L (section 'Effect of initial F^- concentration on ion removal' finding) can be calculated by following the 58% of Mg^{2+} removal. Accordingly minimum of Mg_0^{2+} 75 mg/L was required to treat 4.29 mg/L F_0^- solution to meet the WHO guideline.

With increasing Mg_0^{2+} in the cathode, the removal of $(HCO_3^- + CO_3^{2-})$ was increased gradually and reached a maximum of 45% while $(HCO_3^- + CO_3^{2-})$ removal in the anode was increased marginally (Figure 8(a) and 8(b)). This is clear evidence that the amount of $MgCO_3$ formed in the cathode increased with increasing charge loading. However, lower removal of $(HCO_3^- + CO_3^{2-})$ in the cathode for lower Mg_0^{2+} restricted the system's usability for $(HCO_3^- + CO_3^{2-})$ removal for drinking purposes. The higher removal efficiency of $(HCO_3^- + CO_3^{2-})$ in the anode even at lower Mg_0^{2+} concentration,

H2Open Journal Vol 3 No 1
doi: 10.2166/h2oj.2020.022

proves that anode treated water even at lower Ca_0^{2+} concentration and proves that anode treated water meets both industrial and drinking water quality guidelines.

Effect of initial Ca^{2+} concentration on ion removal and related pH

This section describes the effect of the Ca_0^{2+} concentration on the ion removal under the conditions described in Table 1. After three hours of stabilizing time, the anode and the cathode water out-flow rates were measured. It was found that 2.40, 1.99, 0.51, 0.24, 0, and 0 mL/min flowed through the diaphragm from the anode to the cathode for the initial Ca^{2+} concentrations of 0, 25, 50, 75, 100, and 125 mg/L, respectively. Accordingly, the removal percentage was calculated by accounting for the inflow weight and the outflow weight of the elements for a better comparison. The calculated removal rates against increasing initial Ca^{2+} concentrations are illustrated in Figure 9(a) and 9(b) for the cathode and the anode, respectively. Figure 9(c) shows the pH levels in the anode and the cathode for different Ca_0^{2+} concentrations. No significant

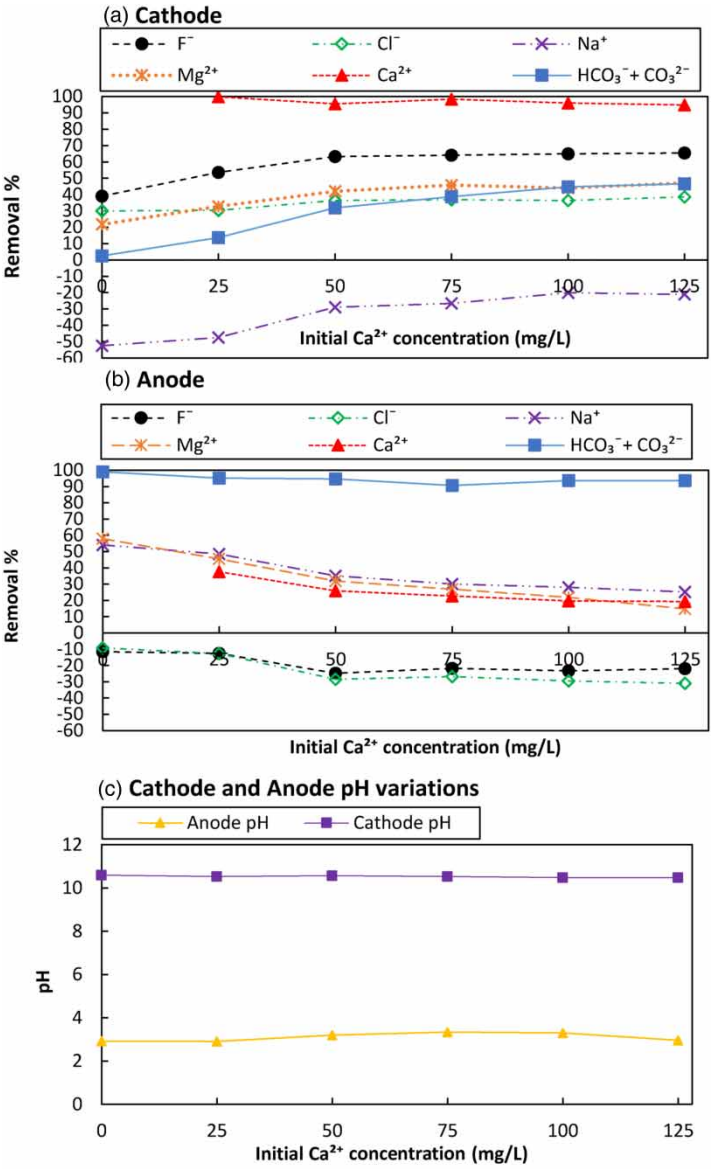

Figure 9 | Influence of the initial Ca^{2+} concentration in the electrolytes on the ion removal percentage and the pH. (a) Cathode, (b) anode, (c) pH variation; $F_0^- = 10$ mg/L, $Ca_0^{2+} = 0$–125 mg/L, $Mg_0^{2+} = 100$ mg/L, and $(HCO_3^- + CO_3^{2-}) = 10$ mmol/L, 1500 C/L.

H2Open Journal Vol 3 No 1
doi: 10.2166/h2oj.2020.022

fluctuation of pH was observed with increasing Ca_0^{2+} in both the anode and the cathode (Figure 9(c)) ensuring the no effect of the Ca^{2+} for OH^- and H^+ consuming reactions were negligible.

According to Figure 9(a), the removal of F^- and Mg^{2+} increased marginally for $Ca_0^{2+} < 50$ mg/L and maximized after $Ca_0^{2+} > 50$ mg/L. Accordingly, the addition of Ca_0^{2+} (0–50 mg/L) contributed to the increment of F^- removal up to 24% (39–63%). On the other hand, with increasing Ca_0^{2+} (0–50 mg/L), removal of F^- increased negatively by 11% (−12% to −23%) in the anode by transferring via the Coulomb force. Hence, the contribution of the Ca_0^{2+} increment from 0 to 50 mg/L for F^- removal was approximately 13%. By accounting for the findings discussed in section 'Effect of initial F^- concentration on ion removal' and this section, for $Ca_0^{2+} > 50$ mg/L and $F_0^- < 4.29$ mg/L, the WHO guideline level of F^- for drinking purposes was attainable in the cathode. According to Figure 9(b), a slight increase in $(HCO_3^- + CO_3^{2-})$ removal in the cathode was observed above the increase in Ca_0^{2+}. Obviously, this has resulted in an increase in the formation of $CaCO_3$ above the increase in Ca_0^{2+} (Lin & Singer 2009). Moreover, the removal of $(HCO_3^- + CO_3^{2-})$ in the cathode increased from 2.4 to 46% (Figure 9(b)). Higher removal efficiency (more than 90%) of $(HCO_3^- + CO_3^{2-})$ in the anode even at lower Ca_0^{2+} concentration, proves that anode treated water meets both industrial and drinking water quality guidelines.

Effect of the initial $HCO_3^- + CO_3^{2-}$ concentration on ion removal and related pH

From the previous section 'Effect of charge loading on ion-removal efficiencies, Effect of the anode flow rate on ion removal, Effect of initial F^- concentration on ion removal, Effect of the initial Mg^{2+} concentration on ion removal and Effect of initial Ca^{2+} concentration on ion removal and related pH' data, the presence of $HCO_3^- + CO_3^{2-}$ significantly alters the removal of Ca^{2+}, Mg^{2+}, and F^-. $HCO_3^- + CO_3^{2-}$ directly involved for the OH^- and H^+ acquisition reactions (Equations (3) and (4)). Therefore, for detail investigation, ion removal at different initial concentrations of $(HCO_3^- + CO_3^{2-})_0$ was studied at 1500 C/L by following the experimental conditions listed in Table 1. The water flow through the diaphragm from the anode to the cathode was found negligible. The calculated removal percentages of ions in the cathode, the anode, and pH values are shown in Figure 10(a)–10(c), respectively. In the absence of $HCO_3^- + CO_3^{2-}$, the removal of F^- and Mg^{2+} increased to 70% in the cathode. The removal of 70% can be observed. Generated OH^- was used only for the formation of $Mg(OH)_2$. Equal positive and negative removal percentages of Ca^{2+} ions in the anode and the cathode further confirmed that there was no possibility of removing Ca^{2+} as a precipitate, even in the form of $Ca(OH)_2$ or CaF_2 in the absence of $(HCO_3^- + CO_3^{2-})$. Therefore, the only mechanism that could remove F^- was co-precipitation with $Mg(OH)_2$. Only 1% of F^- was transferred from the cathode to the anode by the Coulomb force, and 69% was removed by co-precipitation in the cathode (Figure 10(a)). Moreover, with increasing $(HCO_3^- + CO_3^{2-})_0$, F^- transferred to the anode was increased. The ion concentration gradient between the anode and the cathode created by F^- co-precipitation in the cathode seems stronger than the Coulomb force. Therefore, F^- transfer to the anode by the Coulomb force was reduced as $(HCO_3^- + CO_3^{2-})_0$ was reduced. Furthermore, 19% of Mg^{2+} was transferred from the anode to the cathode due to the Coulomb force.

Following the removal percentages of F^- in the cathode, maximum treatable F_0^- concentrations can be calculated as 5–6 mg/L (assuming same 74% removal observed for 10 mg/L F_0^-) to meet WHO guideline for drinking water when $(HCO_3^- + CO_3^{2-})_0$ concentration was lower than 5 mmol/L. The higher removal rate of $(HCO_3^- + CO_3^{2-})$ in the anode more than 90% for $(HCO_3^- + CO_3^{2-})_0 =$ 0–12.5 mmol/L showed that the proposed ELC system would be applicable to removal from both industrial and drinking water $(HCO_3^- + CO_3^{2-})$.

H2Open Journal Vol 3 No 1
doi: 10.2166/h2oj.2020.022

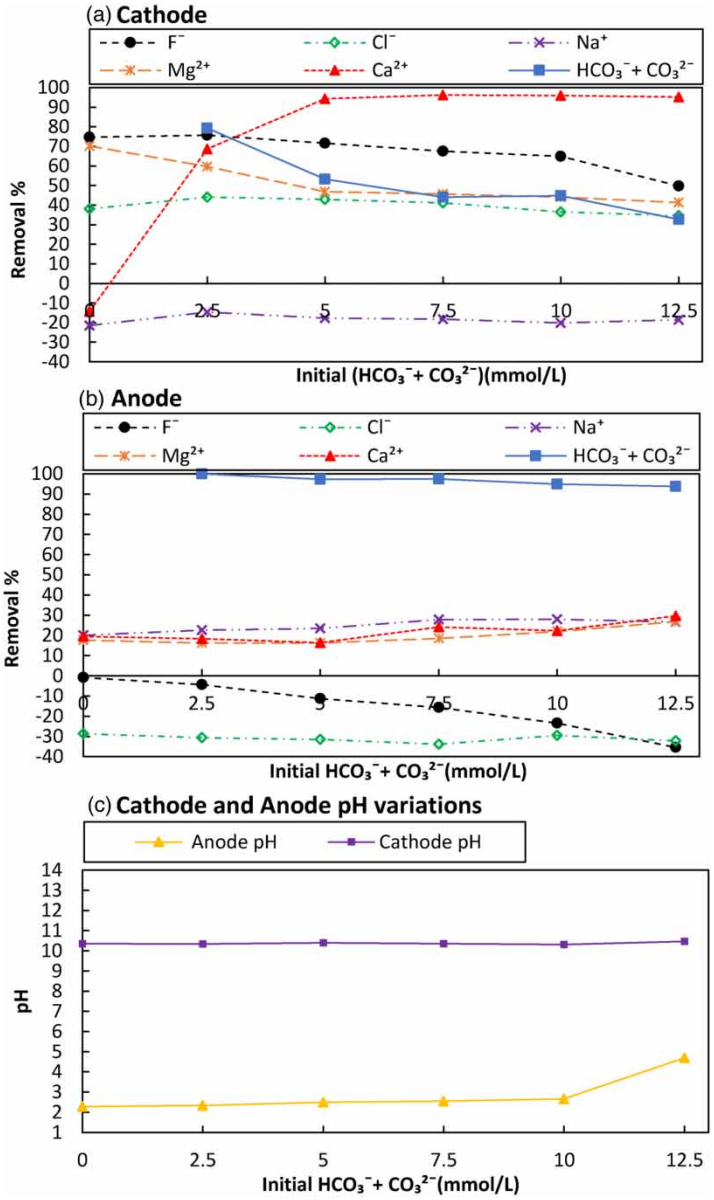

Figure 10 | Influence of initial $HCO_3^- + CO_3^{2-}$ concentration in electrolyte on the ion removal and pH. (a) Cathode, (b) anode, (c) pH variation; $F_0^- = 10$ mg/L, $Ca_0^{2+} = 100$ mg/L, $Mg_0^{2+} = 100$ mg/L, and $(HCO_3^- + CO_3^{2-})_0 = 0$–12.5 mmol/L, 1500 C/L.

Model treatment system and its performance in real conditions

The ELC system was implemented in Sri Lanka as a model treatment system for 5–6 families where there was an urgent need for qualified groundwater for drinking purposes. Accordingly, a groundwater source located in the Medawachchiya area of the Anuradhapura District (location: 8° 32′02.8″N 80°29′57.6″E) of Sri Lanka was selected. The treatment system was established with a production capacity of 374 L/day, having the same retention time of laboratory experiments. The anode water was rejected since the system was utilized for drinking purposes. During the operation, negligible flow through the diaphragm was observed.

The water quality of well water (WW), ion removals in the anode and the cathode are shown in Table 3. According to Table 3, there was a high concentration of F^- in the well water, exceeding the Sri Lankan guideline of 1 mg/L, as well as the WHO guideline of 1.5 mg/L (SLSI 2013; WHO 2017). The concentrations of other ions were also found to be extremely high and did not fluctuate significantly during the operating period except $HCO_3^- + CO_3^{2-}$. Figure 11 shows the charge loading

Table 3 | Well water (WW) quality

	mg/L						mmol/L	
	F^-	Cl^-	SO_4^{2-}	Na^+	Mg^{2+}	Ca^{2+}	$HCO_3^- + CO_3^{2-}$	pH
Avg.	2.71 ± 0.02	2532.71 ± 5.17	602.71 ± 0.96	2052.71 ± 3.32	1312.71 ± 1.85	542.71 ± 1.08	13.82 ± 0.21	7.9V1 ± 0.11
Avg. anode	3.45 ± 0.13	360.00 ± 16.29	87.63 ± 4.28	125.37 ± 10.45	81.71 ± 4.81	33.49 ± 1.65	1.9 ± 0.78	6.45 ± 0.40
Avg. cathode	1.25 ± 0.12	173 ± 12.76	44 ± 2.55	243 ± 7.36	95 ± 11.16	0.1 ± 0.03	11.3 ± 0.59	9.36 ± 0.15
WHO Guideline Limit	**1.50**	**250**	**500**	**200**	**50**	**75**	**6.1**	**8.5**
Sri Lankan Guideline	**1.0**	**1200**	**400**	–	**30**	**240**	**8.0**	**9.0**

H2Open Journal Vol 3 No 1
doi: 10.2166/h2oj.2020.022

H2Open Journal Vol 3 No 1
doi: 10.2166/h2oj.2020.022

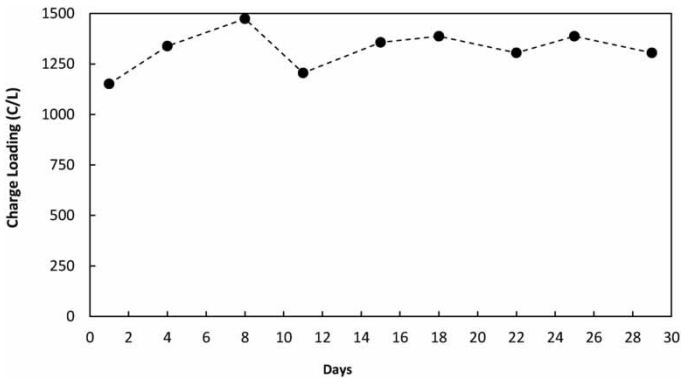

Figure 11 | Charge loading changes in the pilot-scale treatment plant.

applied at the sampling time during 30 days of continuous operation. The charge loading was found to be fluctuated 1152–1474 C/L. The ion removal efficiencies for the cathode, the anode, and related pH are shown in Figure 12(a)–12(c), respectively. According to Figure 12(a), after treatment by the ELC

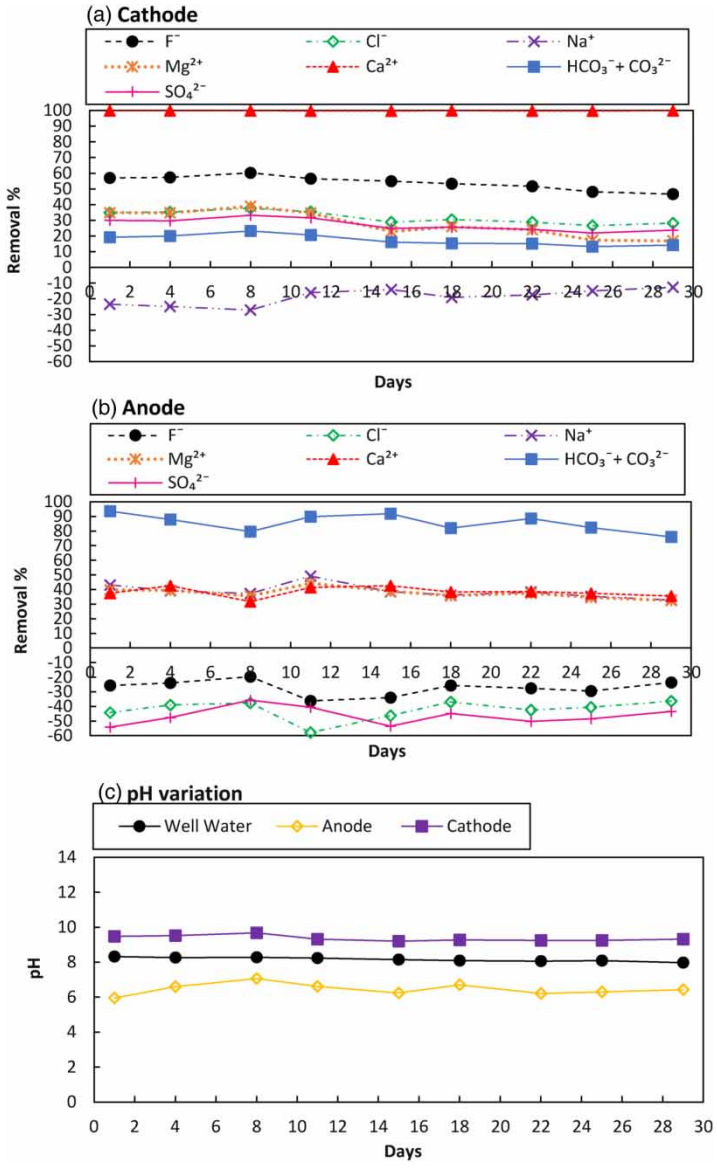

Figure 12 | Ion removal percentage and pH variation of the pilot-scale treatment plant. (a) Cathode, (b) anode, (c) pH variation.

H2Open Journal Vol 3 No 1
doi: 10.2166/h2oj.2020.022

system, the F^- concentration in the cathode was reduced dramatically and was found stable during the operation. The average concentration of F^- in the treated water was 1.25 mg/L, which was less than the WHO guideline. However, F^- and Mg^{2+} removal in the cathode decreased with time which could be caused by the increment of $HCO_3^- + CO_3^{2-}$ concentration over time in the W/W.

The average concentration of Mg^{2+} in the cathode was observed as 81.7 mg/L (27.9% of average removal), which did not meet the WHO guideline of 50 mg/L. This lower removal could be as a result of the high $HCO_3^- + CO_3^{2-}$ concentration in the WW, as described in section 'Effect of the initial $HCO_3^- + CO_3^{2-}$ concentration on ion removal and related pH'. The removal of Ca^{2+} in the cathode was significantly high (>99%), but the removal of $HCO_3^- + CO_3^{2-}$ did not meet the WHO guideline of 6.1 mol/L (Table 3). In the cathode, only F^-, and Ca^{2+} was removed sufficiently to meet the WHO guidelines for drinking water. However, applying higher charge loadings to the system could increase the Mg^{2+}, F^-, and $HCO_3^- + CO_3^{2-}$ removal in both the anode and the cathode to meet WHO and Sri Lankan drinking water quality guidelines. $HCO_3^- + CO_3^{2-}$ removal in the anode was high enough to

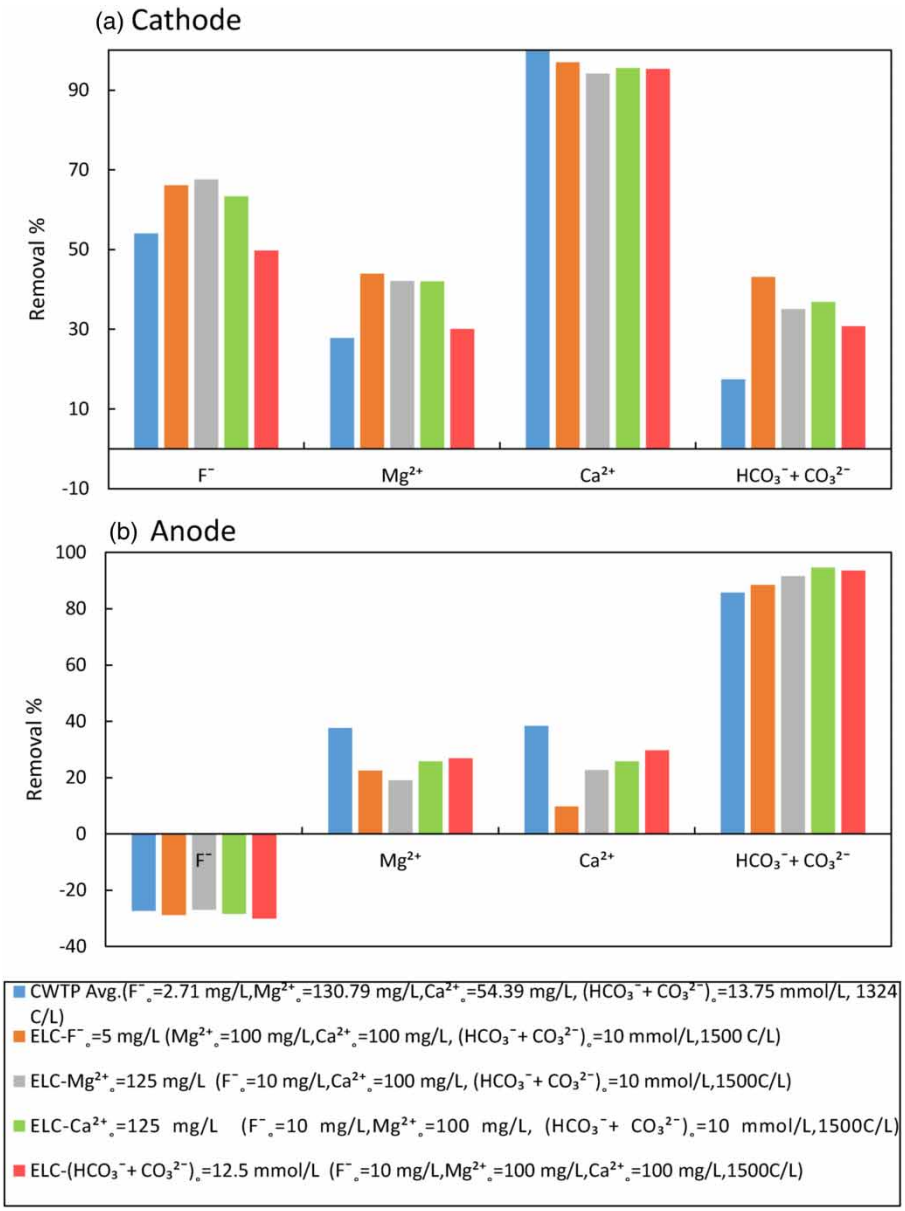

Figure 13 | Comparison of average ions removed in a community-level treatment system with experimental ion removal.

H2Open Journal Vol 3 No 1
doi: 10.2166/h2oj.2020.022

meet the drinking water quality standard of both WHO and Sri Lanka as well as an industrial guideline of 4 mmol/L (Figure 12(b) and Table 3).

Figure 13 compares the average water quality data of the community-level water treatment plant (CWTP) with the experimental data obtained in previous sections 'Effect of initial F^- concentration on ion removal, Effect of the initial Mg^{2+} concentration on ion removal, Effect of initial Ca^{2+} concentration on ion removal and related pH and Effect of the initial $HCO_3^- + CO_3^{2-}$ concentration on ion removal and related pH'. It was observed that the average ion removal of Ca^{2+} in the cathode of CWTP was mostly similar to the laboratory-scale treatment system (Figure 13(a)). However, the removal of F^-, Mg^{2+}, and $CO_3^{2-} + HCO_3^{2-}$ in both anode and cathode was different due to changes in the initial concentrations. Therefore, a rough estimation of the quality of water output based on the initial ion concentration can be performed with laboratory experimental data.

CONCLUSION

A novel method of ELC to remove coexisting F^-, Ca^{2+}, Mg^{2+}, CO_3^{2-}, and HCO_3^- from drinking and industrial groundwater was used without introducing any chemicals. Results were used to set the operational guidelines, to propose the mechanisms of ion removal, and to study the system's operation under real groundwater conditions. The ELC system was found to remove ions satisfactorily. The removal of F^-, Ca^{2+}, and Mg^{2+} in the cathode was found to be significant; thus, cathode outlet water was most suitable for drinking purposes. $(CO_3^{2-} + HCO_3^-)$ removal in the anode as CO_2 was found to be the best and most suitable for industrial purposes. F^- was removed from the cathode mainly by co-precipitation with $Mg(OH)_2$ and by Coulomb force transfer to the anode. The minor adsorptive removal of F^- by $CaCO_3 + MgCO_3$ was also observed. To meet the WHO drinking water guideline levels for F^-, a range of initial ion concentrations was recognized as $F_0^- = 4.29$–6 mg/L, $Mg_0^{2+} = 75$–125 mg/L, $Ca_0^{2+} > 50$ mg/L, and $(HCO_3^- + CO_3^{2-})_0 < 10$ mmol/L in place of 1500 C/L.

ACKNOWLEDGEMENTS

This research was partly supported by JSPS KAKENHI Grant Numbers 23404003 and 15H05120. Furthermore, the authors gratefully acknowledge Prof. Masamoto Tafu, Dept. Appl. Chem. & Chem. Eng., National Institute of Technology, Toyama College, Japan, for providing the XRD analytical facility.

REFERENCES

Amarasooriya, A. A. G. D. & Kawakami, T. 2019 Electrolysis removal of fluoride by magnesium ion-assisted sacrificial iron electrode and the effect of coexisting ions. *J. Environ. Chem. Eng.* **7**, 103084.

Amini, M., Mueller, K., Abbaspour, K. C., Rosenberg, T., Afyuni, M., Møller, K. N., Sarr, M. & Johnson, C. 2008 Statistical modeling of global geogenic fluoride contamination in groundwaters. *Environ. Sci. Technol.* **42**, 3662–3668.

Ayoob, S. & Gupta, A. K. 2006 Fluoride in drinking water: a review on the status and stress effects. *Crit. Rev. Environ. Sci. Technol.* **36** (6), 433–487.

Devi, R. R., Umlong, I. M., Raul, P. K., Das, B., Banerjee, S. & Singh, L. 2012 Defluoridation of water using nano-magnesium oxide. *J. Exp. Nanosci.* **1**, 512–524.

Electric Power Development Co., Ltd, Shikoku Electric Power Co., Inc., West Japan Engineering Consultants, Inc. 2013 *Guideline for Technical Regulation*. Japan International Cooperation Agency, Tokyo.

Gabrielli, C., Maurin, G., Francy-Chausson, H., Thery, P., Tran, T. T. M. & Tlili, M. 2006 Electrochemical water softening: principle and application. *Desalination* **201**, 150–163.

Gascó, G. & Méndez, A. 2005 Sorption of Ca^{2+}, Mg^{2+}, Na^+ and K^+ by clay minerals. *Desalination* **182**, 333–338.

H2Open Journal Vol 3 No 1
doi: 10.2166/h2oj.2020.022

Janson, A., Minier-Matar, J., Al-Shamari, E., Hussain, A., Sharma, R., Adham, S. & Rowley, D. 2018 Evaluation of new ion exchange resins for hardness removal from boiler feedwater. *Emergent Mater.* **1**, 77–87.

Karimi, A., Radfard, M., Abbasi, M., Naghizadeh, A., Biglari, H., Alvani, V. & Mahdavi, M. 2018 Fluoride concentration data in groundwater resources of Gonabad, Iran. *Data Br.* **21**, 105–110.

Kawakami, T., Nishino, M., Imai, Y., Miyazaki, H. & Amarasooriya, A. A. G. D. 2018 De-fluoridation of drinking water by co-precipitation with magnesium hydroxide in electrolysis. *Cogent Eng.* **5**, 1–13.

Ketata, M., Hamzaoui, F., Gueddari, M., Bouhlila, R. & Ribeiro, L. 2011 Hydrochemical and statistical study of groundwaters in Gabes-south deep aquifer (south-eastern Tunisia). *Phys. Chem. Earth* **36**, 187–196.

Kim, K. & Jeong, G. Y. 2005 Factors influencing natural occurrence of fluoride-rich groundwaters: a case study in the southeastern part of the Korean Peninsula. *Chemosphere* **58**, 1399–1408.

Kuokkanen, V., Kuokkanen, T., Rämö, J. & Lassi, U. 2013 Recent applications of electrocoagulation in treatment of water and wastewater – a review. *Green Sustain. Chem.* **03**, 89–121.

Lin, Y. P. & Singer, P. C. 2009 Effect of Mg^{2+} on the kinetics of calcite crystal growth. *J. Cryst. Growth* **312** (1), 136–140.

Luo, W., Gao, X. & Zhang, X. 2018 Geochemical processes controlling the groundwater chemistry and fluoride contamination in the yuncheng basin, China – an area with complex hydrogeochemical conditions. *PLoS One* **13**, 1–25.

Masindi, V., Gitari, W. M. & Ngulube, T. 2015 Kinetics and equilibrium studies for removal of fluoride from underground water using cryptocrystalline magnesite. *J. Water Reuse Desalin.* **5**, 282–292.

Meenakshi & Maheshwari, R. C. 2006 Fluoride in drinking water and its removal. *J. Hazard. Mater.* **137**, 456–463.

Oladoja, N. A., Hu, S., Drewes, J. E. & Helmreich, B. 2016 Insight into the defluoridation efficiency of nano magnesium oxide in groundwater system contaminated with hexavalent chromium and fluoride. *Sep. Purif. Technol.* **162**, 195–202.

Plummer, L. N. & Busenberg, E. 1982 The solubilities of calcite, aragonite and vaterite in CO_2-H_2O solutions between 0 and 90° C, and an evaluation of the aqueous model for the system $CaCO_3$-CO_2-H_2O. *Geochim. Cosmochim. Acta* **46**, 1011–1040.

Rafique, T., Naseem, S., Usmani, T. H., Bashir, E., Khan, F. A. & Bhanger, M. I. 2009 Geochemical factors controlling the occurrence of high fluoride groundwater in the nagar Parkar area, Sindh, Pakistan. *J. Hazard. Mater.* **171**, 424–430.

Rango, T., Kravchenko, J., Atlaw, B., McCornick, P. G., Jeuland, M., Merola, B. & Vengosh, A. 2012 Groundwater quality and its health impact: an assessment of dental fluorosis in rural inhabitants of the Main Ethiopian Rift. *Environ. Int.* **43**, 37–47.

Salifu, A., Petrusevski, B., Ghebremichael, K., Buamah, R. & Amy, G. 2012 Multivariate statistical analysis for fluoride occurrence in groundwater in the Northern region of Ghana. *J. Contam. Hydrol.* **140–141**, 34–44.

Shen, J. & Schafer, A. 2014 Removal of fluoride and uranium by nanofiltration and reverse osmosis: a review. *Chemosphere* **117** (1), 679–691.

Singaraja, C., Chidambaram, S., Anandhan, P., Prasanna, M. V., Thivya, C., Thilagavathi, R. & Sarathidasan, J. 2014 Geochemical evaluation of fluoride contamination of groundwater in the Thoothukudi District of Tamilnadu, India. *Appl. Water Sci.* **4**, 241–250.

SLSI 2013 Sri Lanka Standards for potable water-(SLS 614). In: *Drinking Water Standards*. Sri Lankan Standards Institute, Colombo.

Su, C., Wang, Y., Xie, X. & Li, J. 2013 Aqueous geochemistry of high-fluoride groundwater in Datong Basin, Northern China. *J. Geochemical Explor.* **135**, 79–92. 3.

Thapa, R., Gupta, S., Gupta, A., Reddy, D. V. & Kaur, H. 2018 Geochemical and geostatistical appraisal of fluoride contamination: an insight into the Quaternary aquifer. *Sci. Total Environ.* **640–641**, 406–418.

Turner, B. D., Binning, P. & Stipp, S. L. S. 2005 Fluoride removal by calcite: evidence for fluorite precipitation and surface adsorption. *Environ. Sci. Technol.* **39**, 9561–9568.

WHO 2017 *Guidelines for Drinking–Water Quality: Fourth Edition Incorporating the First Addendum*, 4th edn. World Health Organization, Geneva.

Wickramarathna, S., Balasooriya, S., Diyabalanage, S. & Chandrajith, R. 2017 Tracing environmental aetiological factors of chronic kidney diseases in the dry zone of Sri Lanka – a hydrogeochemical and isotope approach. *J. Trace Elem. Med. Biol.* **44**, 298–306.

Zeppenfeld, K. 1998 Electrolysis as a method for partial decarbonisation. *GWF Wasser-Abwasser* **139** (1), 86–91.

Zeppenfeld, K. 2011 Electrochemical removal of calcium and magnesium ions from aqueous solutions. *Desalination* **277** (1–3), 99–105.

Zhi, S. & Zhang, K. 2016 Hardness removal by a novel electrochemical method. *Desalination* **381**, 8–14.

First received 14 October 2019; accepted in revised form 3 February 2020. Available online 9 March 2020